RSC Advances

PAPER

View Article Online
View Journal | View Issue

Cite this: *RSC Adv.*, 2017, **7**, 41869

Synthesis, cytotoxic evaluation and DNA binding study of 9-fluoro-6*H*-indolo[2,3-*b*]quinoxaline derivatives†

Zhenyu Gu, Yanci Li, Songliang Ma, Shenghui Li,* Guoqiang Zhou,* Shan Ding, Jinchao Zhang, Shuxiang Wang and Chuanqi Zhou

A series of novel 9-fluoro-6*H*-indolo[2,3-*b*]quinoxaline derivatives as antitumor agents were synthesized and studied. The designed compounds feature positive charges both at the 11-*N* position of the aromatic scaffold and the side-chain alkylamino group. The corresponding *in vitro* antitumor activities were evaluated against MCF-7, HeLa and A549 cancer cell lines and the DNA binding properties of these compounds were characterized by UV-vis, fluorescence, and circular dichroism (CD) spectroscopy as well as thermal denaturation. The obtained results indicate that the dicationic quaternary ammonium salt derivatives of 9-fluoro-6*H*-indolo[2,3-*b*]quinoxaline may serve as intercalators with increased DNA binding affinity. Furthermore, both the incorporation of fluorine, and alkyl amino side chains and the introduction of a positive charge at the 11-*N* position of the aromatic scaffold was shown to be responsible for their antitumor activity and improved DNA binding ability. Taken in concert, these findings may be valuable in the understanding of the antitumor effect of these compounds and may further provide important information for the future optimization of the DNA binding properties of this drug type.

Received 24th July 2017
Accepted 21st August 2017

DOI: 10.1039/c7ra08138c

rsc.li/rsc-advances

1. Introduction

As the second leading cause of death worldwide, cancer accounts for nearly one in four of all mortality cases. It is estimated that about 10 million new cancer cases are diagnosed every year, causing a major health concern in both the developing and the developed countries.[1] Despite advances in surgery and radiation therapy, chemotherapy still plays a crucial role in cancer treatment. However, the overall chemotherapeutic success is still limited by several drawbacks, including inadequate drug concentrations at the tumor site, undesirable toxicity, poor tumor cell selectivity over normal cells, and the occurrence of multiple drug resistance.[2,3] Therefore, the discovery and development of selective, efficient, and safe drug types for anticancer chemotherapy remains a critical goal with high priority in medical research.

Modification of existing active drug candidates, known as analogue design, is one of the most widely accepted approaches in drug discovery for the development of new drugs and improved therapeutic properties.[4–9] Natural alkaloids and alkaloid derivatives, such as indoloquinoline alkaloid cryptolepine and pyridocarbazole alkaloid ellipticine, have attracted considerable attention due to their interesting biological activities demonstrated by both *in vitro* and *in vivo* studies. Their antitumor, mutagenic and cytotoxic activities were found to be due to a variety of mechanisms, including (i) DNA intercalation, (ii) inhibition of DNA topoisomerase II activity, and others.[10] Unfortunately, toxicity issues have more or less limited the overall success of these drugs in pharmaceutical industry.[11]

In recent years, 6*H*-indolo[2,3-*b*]quinoxaline (*cf.* Fig. 1) have received much attention due to its important pharmacological activities, including antiviral (herpes simplex virus type 1 (HSV-1), cytomegalovirus (CMV), varicellazoster virus (VZV), *etc.*), cytotoxic and multidrug resistant (MDR) modulating activities, acting on ATP binding cassette transporters (ABC-transporters).[12,13] 6*H*-Indolo[2,3-*b*]quinoxaline combines the structural features of indoles and quinoxalines and may be regarded as an aza-analogue of the cytotoxic agents cryptolepine and ellipticine.[14] The planar structure of this compound aids in the intercalation of DNA which in turn is responsible for biological activities such as cytotoxicity, antiviral activity, *etc.*[12,13] The compound class has been well-studied and well-described in the literature, primarily by Bergman and co-workers.[15–18] In recent years, several analogues of 6*H*-indolo[2,3-*b*]quinoxaline have been synthesized, *e.g.* B-220 (2,3-dimethyl-6-(2-dimethylaminoethyl)-6*H*-indolo[2,3-*b*]quinoxaline, Fig. 1), NCA0424, and

Key Laboratory of Chemical Biology of Hebei Province, Key Laboratory of Medicinal Chemistry and Molecular Diagnosis, Ministry of Education, College of Chemistry & Environmental Science, Hebei University, Baoding 071002, China. E-mail: lish@hbu.cn; zhougq1982@163.com; Fax: +86 0312 5079005; Tel: +86 0312 5079005

† Electronic supplementary information (ESI) available. CCDC 1541589. For ESI and crystallographic data in CIF or other electronic format see DOI: 10.1039/c7ra08138c

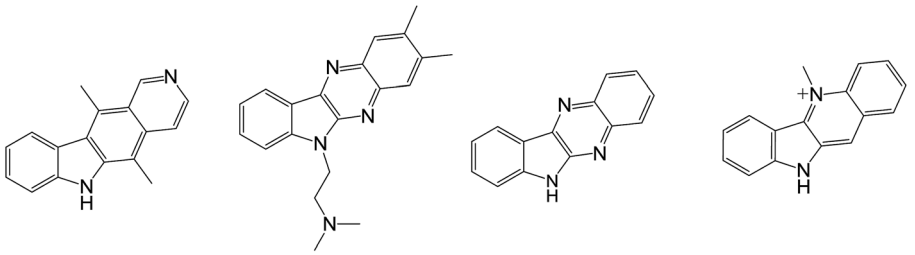

Fig. 1 The structure of ellipticine, B-220, indolo[2,3-*b*]quinoxaline and cryptolepine.

others. Importantly, these compounds exhibited high antiviral activity and selective anticancer activity (Fig. 1).[19–24] Hence, the indolo[2,3-*b*]quinoxaline nucleus was considered as a template for the design and development of DNA intercalating agents with cytotoxic activities in this study.

Owing to the special nature of fluorine as a functional group, the incorporation of fluorine usually conveys a variety of properties to certain pharmaceuticals and includes enhanced binding interactions, metabolic stability, changes in physical properties, and selective reactivities.[25] Today, fluorine is present in up to 30% of pharmaceuticals. More recently, Karki *et al.* reported that 9-fluoro-6-(4-methylbenzyl)-6*H*-indolo[2,3-*b*]quinoxaline exhibited a potent anticancer activity against various human tumor cell lines.[26] Meanwhile, it is generally appreciated that the transformation of neutral chromophores into their cationic derivatives usually enhances their affinity for DNA, thus increasing the overall antitumor activity.[27,28] This is also the case for elliptinium, a cationic derivative of 9-methoxyellipiticine.[29,30] Apart from the contribution of planar polycyclic aromatic systems, higher DNA binding affinity and biological activities may also be affected by the introduction of substituted groups such as amino side chains,[11,31–34] sugars,[35,36] or heterocycles[37,38] to the chromophore. Furthermore, a cationic amino side chain may play an important role in the increase of the DNA binding affinity and biological activities due to their electrostatic interaction with the phosphate moieties of DNA. Moreover, chains of varying length, different polarity, structural rigidity, charge and steric bulk may also result in different DNA binding affinities.[39]

This work was designed to synthesize and study a group of novel 9-fluoro-6*H*-indolo[2,3-*b*]quinoxaline derivatives with improved DNA binding affinity and antitumor activity by attaching various alkyl amino side chains to the chromophore and introducing multiple positive charges *via* selective methylation at the nitrogens of the quinoxaline ring and the terminal amino-group. The DNA binding affinity of the resulting 9-fluoro-6*H*-indolo[2,3-*b*]quinoxaline derivatives was evaluated based on interaction with calf thymus (CT) DNA and the cytotoxicity of the compounds was assessed on three types of tumor cell lines, human mammary cancer (MCF-7) cells, human cervical carcinoma (HeLa) cells, and human lung cancer (A549) cells. Furthermore, the molecular structure and bioactivity relationships of the compounds were studied as discussed in subsequent sections.

2. Results and discussion

2.1. Synthesis and characterization

The synthesis of the quaternary mono- or dicationic indoloquinoxaline derivatives was carried out as depicted in Scheme 1. Isatin was obtained from commercial sources. 5-Fluoroisatin was synthesized according to a published procedure.[40] 9-Fluoro-6*H*-indolo[2,3-*b*]quinoxaline (**2a**) and 6*H*-indolo[2,3-*b*]quinoxaline (**2d**) were prepared by condensation of 5-fluoroisatin (or isatin) with 1,2-phenylenediamine in glacial acetic acid according to a procedure reported previously.[41] The key intermediates of 6-bromoalkyl indolo[2,3-*b*]quinoxaline **3** were synthesized *via* alkylation by the use of excess dibromoalkane in tetrahydrofuran (THF) in the presence of potassium hydroxide. Amination using the corresponding cyclic secondary amines access lead to aminoalkyl-indoloquinoxalines **4**. The methylation of **4** with iodomethane in different solvents (acetone or tetramethylenesulfone) selectively afforded the mono- or dicationic fluorinated indoloquinoxaline derivatives in excellent yield.[42]

The structures of the target compounds were characterized by IR spectroscopy, mass-spectrometry, NMR-spectroscopy, and single crystal X-ray diffraction analysis of the precursor of compound **6b-1**. Vibrations of aromatic C–H bonds were observed in the IR spectra of the obtained compounds at 3096–3035 cm^{-1}, with aliphatic signals appearing at 2980–2753 cm^{-1}. Double bond vibrations of heterocyclic fragments exhibited a band at 1621–1450 cm^{-1}. The bands at 1236–1058 cm^{-1} corresponded to CH_2–N vibrations. The mass spectra displayed the correct molecular ion peaks and the measured high resolution (HRMS) data was also in good agreement with the calculated values.

Two "parts" corresponding to the aromatic and aliphatic moieties of the molecules were observed in ^1H NMR-spectra of the synthesized indoloquinoxalines derivatives. The spectral ranges for the aliphatic regions were different due to the presence of terminal amino groups. In the ^{13}C NMR spectrum of the 9-fluoro-6*H*-indolo[2,3-*b*]quinoxaline derivatives, the carbons in the fluorinated aromatic ring resonated as doublets due to spin–spin coupling with the fluorine atom. The carbon–fluorine spin–spin coupling constants of $^1J_{CF}$, $^2J_{CF}$, $^3J_{CF}$ and $^4J_{CF}$ have been determined as 234.0–240.0 Hz, 22.0–25.5 Hz, 9.0–10.5 Hz and 3.0–4.5 Hz, respectively.

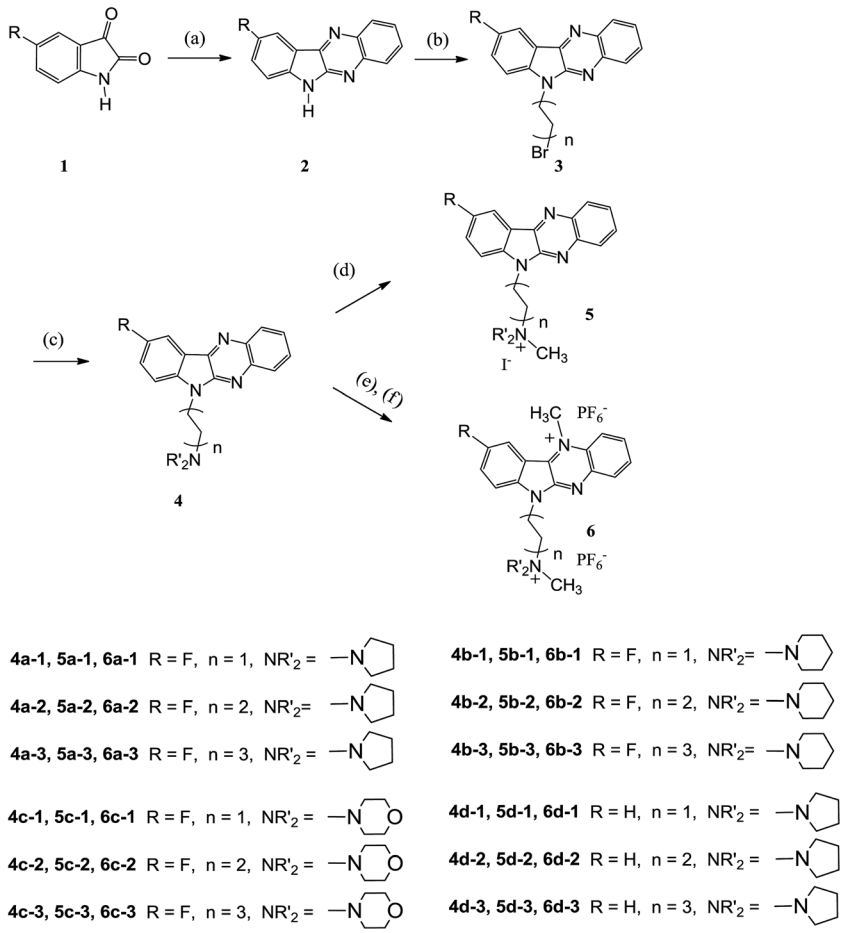

Scheme 1 Synthesis of 9-fluoro-6*H*-indolo[2,3-*b*]quinoxaline derivatives. Reaction conditions: (a) *o*-phenylenediamine, acetic acid, reflux, 5 h; (b) dibromoalkane, KOH, THF, reflux, 6 h; (c) cyclic secondary amine, THF, reflux, N_2; (d) CH_3I, acetone; (e) CH_3I, tetramethylenesulfone, 55 °C, overnight: (f) KPF_6, H_2O, 45 °C, 2 h.

Table 1 Crystallographic data for the precursor of **6b-1**

Formula	$C_{23}H_{29}FI_2N_4O$
F_w	650.30
T (K)	296(2)
Cryst syst	Triclinic
Space group	$P\bar{1}$
a (Å)	7.840(3)
b (Å)	12.067(5)
c (Å)	14.220(6)
V (nm^3)	1312.3(9)
Z	2
D_c (Mg m^{-3})	1.646
F (000)	636
Cryst dimens (mm)	0.35 × 0.15 × 0.13
θ Range (deg)	2.18–26.00
hkl ranges	$-9 < h < 7$
	$-14 < k < 14$
	$-17 < l < 15$
Data/parameters	5085/290
Goodness-of-fit on F^2	1.072
Final R indices [$I > 2\sigma(I)$]	$R_1 = 0.0342$
	w$R_2 = 0.0831$

2.2. Structural studies

An X-ray crystal structure determination was performed to confirm the structure of the precursor of **6b-1** in the solid phase. A summary of data collection and refinement parameters is provided in Table 1. Based on crystallographic data, the molecular structure of the precursor of compound **6b-1** is shown in Fig. 2. The molecule adopted an almost planar configuration with the piperidinyl ring in the expected chair conformation. The dihedral angle between the two planes intersecting along the *N*,*N*-axis in *N*,*N*-dihydropyrazine was 0.0038° (109). The position of methylation on the nucleus was unambiguously observed at N3 instead of N2. Another methylated position was found at N4. The bond length of N3–C23 was 1.4738 Å (60), while the bond length of N4–C22 was 1.510 Å (6) and the bond length of C4–F1 was 1.3761 Å (43) (Table 2).

2.3. Cytotoxicity studies

The antitumor activities of aminoalkyl-indoloquinoxalines **4** as well as the quaternary mono- and dicationic indoloquinoxaline derivatives **5** and **6** were evaluated *in vitro* against tumor cell lines MCF-7, HeLa and A549, respectively, as listed in Tables

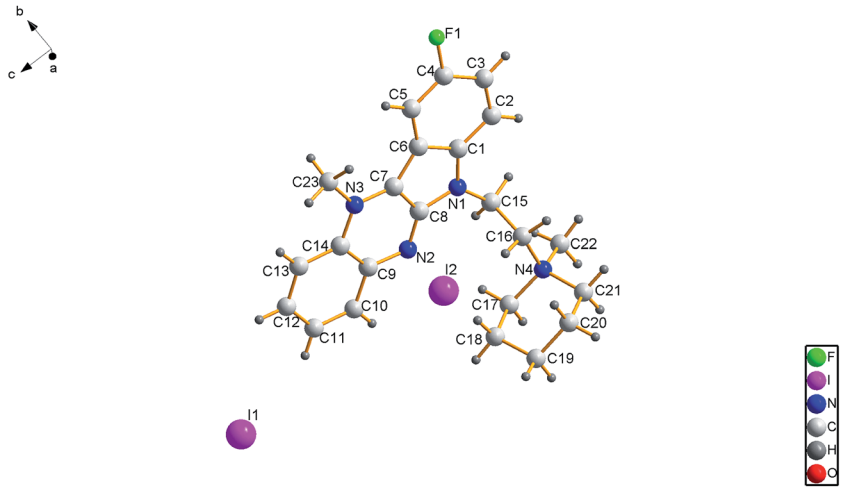

Fig. 2 ORTEP view of the precursor of **6b-1**.

3–5. 9-Fluoro-6*H*-indolo[2,3-*b*]quinoxaline (FIQX) and cisplatin were used as positive controls. According to the data shown in Tables 3–5, most of the synthesized quaternary dicationic FIQX derivatives were found to be more active than the corresponding quaternary monocationic FIQX derivatives and the neutral 6*H*-indolo-[2,3-*b*]quinoxaline derivatives.

As shown in Table 3, most of the neutral 6*H*-indolo[2,3-*b*] quinoxaline derivatives with various alkyl amino side chains showed promising cytotoxicity properties against the tested carcinoma cell lines with low IC_{50} values. Compounds, which contain pyrrolidine as terminal amino-group, *i.e.* compound **4a-1**, **4a-2** and **4a-3**, exhibited potent antiproliferative activities, comparable to the compounds containing piperidinyl and morpholinyl as terminal amino group. Besides, the introduction of fluorine into the aromatic core of 6*H*-indolo [2,3-*b*]quinoxaline seems to enhance the antiproliferative activities of the corresponding compounds as judged by a comparison of the fluorinated indoloquinoxaline derivatives **4a-1**, **4a-2** and **4a-3** as well as the non-fluorinated compounds **4d-1**, **4d-2** and **4d-3**.

As for the monocationic quaternary ammonium salts of 6*H*-indolo[2,3-*b*]quinoxaline (**5**), the *N*-methylation of the terminal amino-group resulted in an apparent decrease of cytotoxicity against MCF-7, HeLa and A549 cells, except for compound **5c-1**.

As for the dicationic quaternary ammonium salts of 6*H*-indolo[2,3-*b*]quinoxaline, the preliminary results demonstrated that most of the compounds were more toxic against MCF-7 than HeLa and A549 cells. Firstly, this compound series exhibited potent antiproliferative activities compared to the corresponding monocationic quaternary ammonium salts derivatives of 6*H*-indolo[2,3-*b*]quinoxaline. For example, compounds **6a-3**, **6b-3** and **6c-3** exhibited an increased antiproliferative activity against MCF-7, with IC_{50} values of 1.80, 1.60 and 3.01 μM, while IC_{50} values for **5a-3**, **5b-3** and **5c-3** of 16.12, 12.45 and 19.19 μM were determined, respectively. It may

Table 2 Selected bond lengths and angles for the precursor of **6b-1**

Length/Å or angle/°			
F(1)–C(4)	1.376(5)	C(5)–C(4)–F(1)	118.2(4)
N(1)–C(8)	2.281(4)	F(1)–C(4)–C(3)	117.1(4)
N(2)–C(8)	1.310(5)	C(8)–N(1)–C(1)	108.9(3)
N(2)–C(9)	1.360(5)	C(8)–N(2)–C(9)	114.5(3)
N(3)–C(7)	1.343(4)	C(7)–N(3)–C(23)	119.3(3)
N(3)–C(14)	1.399(5)	C(7)–N(3)–C(14)	119.0(3)
N(3)–C(23)	1.473(5)	C(14)–N(3)–C(23)	121.7(3)
N(4)–C(22)	1.510(5)	C(17)–N(4)–C(16)	112.6(3)
N(4)–C(17)	1.520(5)	C(22)–N(4)–C(21)	108.3(3)
N(4)–C(16)	1.521(5)	C(17)–N(4)–C(21)	110.1(3)
N(4)–C(21)	1.526(5)	C(22)–N(4)–C(16)	109.6(3)

Table 3 The cytotoxicity of series of compounds (**4**) against MCF-7, Hela and A549

	IC_{50} (μM)[a]		
Compounds	MCF-7	Hela	A549
4a-1	3.68 ± 0.36	5.69 ± 0.48	4.32 ± 0.57
4a-2	8.11 ± 0.52	7.65 ± 1.24	6.36 ± 0.88
4a-3	4.76 ± 0.31	4.25 ± 0.59	4.13 ± 0.33
4b-1	45.58 ± 5.99	19.38 ± 2.10	25.70 ± 3.53
4b-2	34.33 ± 4.65	13.14 ± 1.46	9.01 ± 0.89
4b-3	28.89 ± 3.37	8.61 ± 1.38	10.23 ± 1.05
4c-1	42.68 ± 4.76	27.72 ± 3.48	53.41 ± 6.64
4c-2	11.85 ± 0.98	15.76 ± 1.04	15.00 ± 2.21
4c-3	5.48 ± 0.43	15.49 ± 2.11	19.70 ± 1.98
4d-1	3.69 ± 0.32	6.63 ± 0.55	4.36 ± 0.29
4d-2	10.50 ± 1.76	16.97 ± 2.10	7.45 ± 0.68
4d-3	6.44 ± 0.65	9.58 ± 1.03	3.38 ± 0.44
FIQX	15.44 ± 1.46	20.83 ± 2.22	24.99 ± 3.19
Cisplatin	8.25 ± 0.53[b]	11.06 ± 1.08[c]	8.61 ± 0.39[d]

[a] IC_{50} values were calculated from the linear regression of the dose–log response curves. Values are mean ± S.D. of at least three independent experiments. [b] Ref. 43. [c] Ref. 44. [d] Ref. 45.

Table 4 The cytotoxicity of series of compounds (**5**) against MCF-7, Hela and A549

	IC_{50} (μM)[a]		
Compounds	MCF-7	Hela	A549
5a-1	22.31 ± 3.12	22.64 ± 2.43	20.28 ± 3.04
5a-2	31.57 ± 3.67	23.86 ± 2.75	75.99 ± 6.98
5a-3	16.12 ± 1.31	30.43 ± 3.66	17.82 ± 2.15
5b-1	29.65 ± 3.34	22.88 ± 4.02	17.83 ± 1.60
5b-2	16.58 ± 0.89	24.96 ± 3.57	16.78 ± 2.31
5b-3	12.45 ± 0.81	27.28 ± 2.64	16.25 ± 1.42
5c-1	12.92 ± 1.34	18.09 ± 1.73	12.33 ± 0.51
5c-2	14.38 ± 2.21	30.77 ± 4.03	22.35 ± 2.59
5c-3	19.19 ± 1.47	21.62 ± 2.85	26.84 ± 3.07
5d-1	8.70 ± 0.82	8.56 ± 0.67	7.80 ± 1.20
5d-2	14.75 ± 2.18	9.21 ± 0.62	12.81 ± 0.97
5d-3	8.66 ± 0.42	10.31 ± 1.23	11.41 ± 0.86
FIQX	15.44 ± 1.46	20.83 ± 2.22	24.99 ± 3.19
Cisplatin	8.25 ± 0.53[b]	11.06 ± 1.08[c]	8.61 ± 0.39[d]

[a] IC_{50} values were calculated from the linear regression of the dose–log response curves. Values are mean ± S.D. of at least three independent experiments. [b] Ref. 43. [c] Ref. 44. [d] Ref. 45.

Table 5 The cytotoxicity of series of compounds (**6**) against MCF-7, Hela and A549

	IC_{50} (μM)[a]		
Compounds	MCF-7	Hela	A549
6a-1	3.14 ± 0.33	5.05 ± 0.41	6.31 ± 0.70
6a-2	3.54 ± 0.26	3.87 ± 0.35	5.68 ± 0.42
6a-3	1.80 ± 0.24	4.22 ± 0.63	5.25 ± 0.39
6b-1	2.89 ± 0.38	4.08 ± 0.37	6.09 ± 0.91
6b-2	1.94 ± 0.29	6.04 ± 0.67	8.45 ± 1.28
6b-3	1.60 ± 0.31	3.34 ± 0.55	6.86 ± 1.30
6c-1	7.23 ± 1.06	4.73 ± 0.49	6.82 ± 0.88
6c-2	4.47 ± 0.57	10.43 ± 1.38	6.96 ± 0.59
6c-3	3.01 ± 0.25	8.31 ± 0.66	9.70 ± 0.74
6d-1	3.73 ± 0.44	22.15 ± 2.61	13.33 ± 1.81
6d-2	3.99 ± 0.35	16.12 ± 1.55	9.34 ± 1.02
6d-3	2.02 ± 0.30	9.69 ± 0.77	6.20 ± 0.67
FIQX	15.44 ± 1.46	20.83 ± 2.22	24.99 ± 3.19
Cisplatin	8.25 ± 0.53[b]	11.06 ± 1.08[c]	8.61 ± 0.39[d]

[a] IC_{50} values were calculated from the linear regression of the dose–log response curves. Values are mean ± S.D. of at least three independent experiments. [b] Ref. 43. [c] Ref. 44. [d] Ref. 45.

be concluded that *N*-methylation at 11-position of the indoloquinoxaline ring is essential for the cytotoxicity of 6*H*-indolo[2,3-*b*]quinoxaline derivatives. Secondly, the fluorinated dicationic quaternary ammonium salts of 6*H*-indolo[2,3-*b*]quinoxaline also showed an increased activity compared to the non-fluorinated derivatives. For example, the IC_{50} values of compounds **6a-1**, **6a-2** and **6a-3** were 3.14, 3.54 and 1.80 μM, while the IC_{50} values of compounds **6d-1**, **6d-2** and **6d-3** were 3.73, 3.99 and 2.02 μM, respectively. Additionally, the fluorinated dicationic quaternary ammonium salt derivatives **6a–6c** exhibited higher activities than cisplain against all tested cell lines, however, compound **6c-3** proved to be an exception. Thirdly, the anti-tumor activity results against MCF-7 cells suggested that the dicationic quaternary ammonium salts of 6*H*-indolo[2,3-*b*]quinoxaline with the largest alkyl chains, such as compounds **6a-3**, **6b-3**, **6c-3** and **6d-3**, were more active than compounds with shorter alkyl chains as linkers attached between the terminal amino group and the indolo[2,3-*b*]quinoxaline nucleus.

2.4. DNA-binding property

To evaluate the DNA-binding properties of the cryptolepine analogues, UV-vis absorption spectra, fluorescent spectra, and circular dichroism (CD) spectra were recorded and a thermal denaturation study of the selected compounds **5a-1**, **5a-2**, **6a-1**, **6d-1** and **6b-3** was carried out with CT DNA.

2.4.1. UV-vis titration. UV-vis spectroscopy, based on the absorption of photons of monochromatic light, is one of the most useful techniques to study the binding affinity of a given drug to DNA. Fig. 3 shows the absorption spectra of compounds **5a-1**, **5a-2**, **6a-1**, **6d-1** and **6b-3** in the presence of increasing amounts of CT DNA. It is worthwhile to note that a significant hypochromic effect as well as a red-shift of the absorption maxima could be observed in the spectra of compounds **5a-1**, **5a-2**, **6a-1**, **6d-1** and **6b-3**. These are common effects observed when drugs bind to DNA by either intercalation or groove binding.[11] The large hypochromic effect (29–50%) and red-shift (6–11 nm) displayed by these drugs generally suggest that intercalation is the favored binding mode, but it is also conceivable that electrostatic binding between the negatively charged DNA phosphate backbone and cationic or positive end of these compounds exist at the same time.

To further evaluate and compare the DNA binding performance of these compounds, the binding constants were determined from the following equation:

$$[DNA]/(\varepsilon_a - \varepsilon_f) = [DNA]/(\varepsilon_b - \varepsilon_f) + 1/K_b(\varepsilon_b - \varepsilon_f)$$

where [DNA] is the concentration of DNA in base pairs, ε_a, ε_f and ε_b correspond to average molar extinction coefficient of the solution ($A_{obsd/[compound]}$), molar extinction coefficient of free compound, and molar extinction coefficient of completely bound compound, respectively. K_b represents the intrinsic binding constant. A linear fit of the plot of $[DNA]/(\varepsilon_a - \varepsilon_f)$ *versus* [DNA] provides a slope of $1/(\varepsilon_b - \varepsilon_f)$ and an intercept of $1/K_b(\varepsilon_b - \varepsilon_f)$. K_b could be calculated. The binding constants of the compounds with CT DNA were obtained and found to be $3.33 \times 10^4\ M^{-1}$, $1.67 \times 10^4\ M^{-1}$, $3.50 \times 10^5\ M^{-1}$, $1.42 \times 10^5\ M^{-1}$, $2.34 \times 10^5\ M^{-1}$, respectively. It was found that the DNA binding constants of the monocationic quaternary ammonium salts of 6*H*-indolo[2,3-*b*]quinoxaline derivatives are in the order of 10^4, while that of the dicationic quaternary ammonium salts are in the order of 10^5. This suggests that *N*-methylation at 11-position of the indoloquinoxaline ring enhanced the binding ability of the compounds with DNA. This finding may also be attributed to the double-advantage of *N*-methylated aza-aromatic moieties, *i.e.* increasing the π stacking ability of the ligand due to the reduction of the electron density of the aromatic part and the introduction of a steadily positive charge for the electrostatic

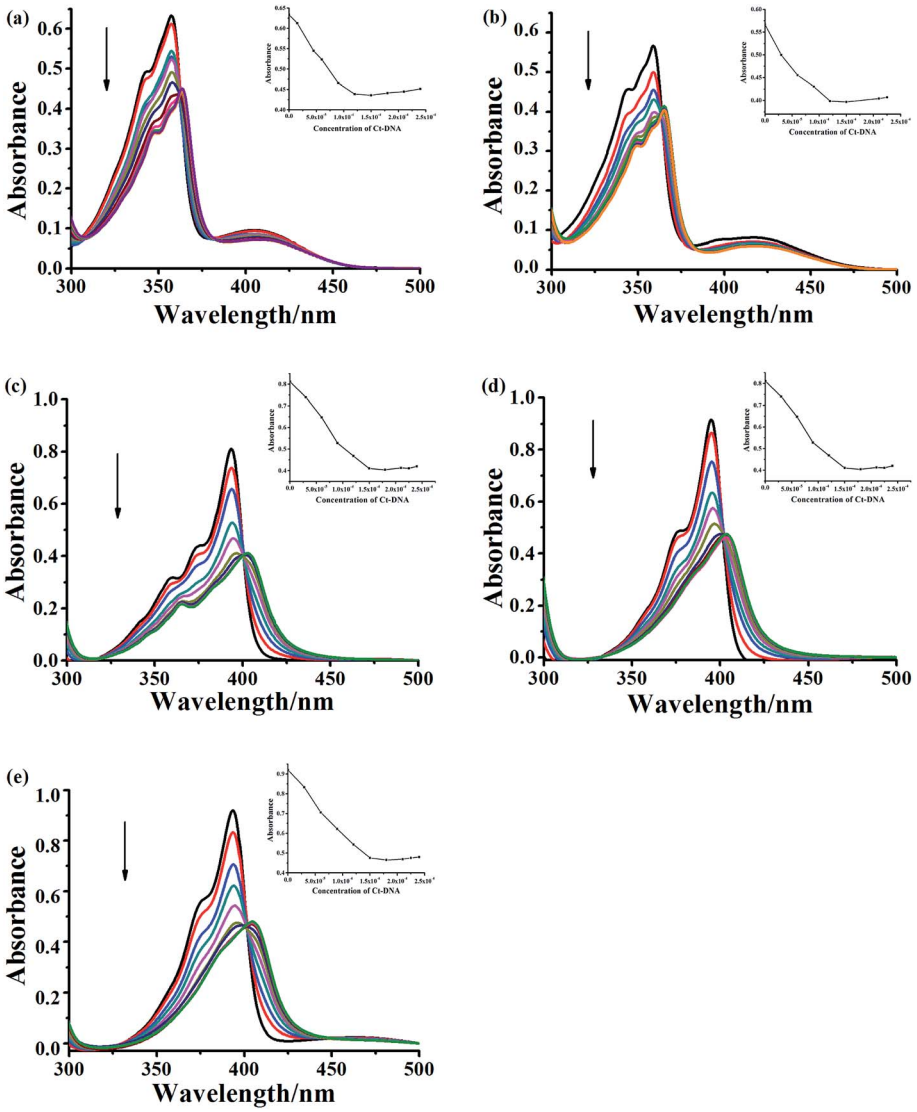

Fig. 3 UV-vis spectral changes of compound **5a-1** (a), **5a-2** (b), **6a-1** (c), **6d-1** (d) and **6b-3** (e) at the concentration of 3.0×10^{-5} M upon addition of CT DNA (arrow: 0–210 μM) in phosphate buffer (1 mM, pH 7.4) containing 20 mM NaCl at 25 °C.

interaction.[46] Taking this latter notion into consideration, the dicationic quaternary ammonium salts of 6*H*-indolo[2,3-*b*]quinoxaline derivatives exhibited a remarkably high binding constant to DNA, which may explain their high antitumor activity compared to monocationic quaternary ammonium salts.

In addition, other variation in the structure, such as the linker length, terminal amino-group and introduction of fluorine atom in the indoloquinoxaline moiety, are shown to have an immediate significant influence on the DNA binding ability. For monocationic quaternary ammonium salts, the binding constants decrease as the linker length increases (**5a-1** > **5a-2**). The compounds with pyrrolidine at the end of side chain show more stronger CT DNA binding affinity than that of compound decorated with piperidine (**6a-1** > **6b-3**). The introduction of fluorine atom into the aromatic core could also enhance DNA binding affinity (**6a-1** > **6d-3**).

2.4.2. Fluorescence property. To gain insights into the binding mode of compounds **5a-1** and **5a-2** with CT DNA, fluorescence titration experiments were performed. Fig. 4 shows the emission spectra of the two compounds in the absence and presence of varying amounts of CT DNA. The results show that the emission intensities of compounds **5a-1** and **5a-2** increased with increasing the CT-DNA concentration, and the wavelength showed a distinct blue shift, similar to the classical model of ethidium bromide (EB) intercalating in DNA.[47] An emission increase upon binding to DNA is often considered to be a good indicator for intercalation of the drug between the DNA base pairs, and thus, these measurements support an intercalative binding mode of **5a-1** and **5a-2** with CT DNA.

2.4.3. Circular dichroism (CD). The difference in absorption of polarised light provides the foundation of recording a CD spectrum. From the changes in the CD of DNA and the induced circular dichroism (ICD) of the compounds, the

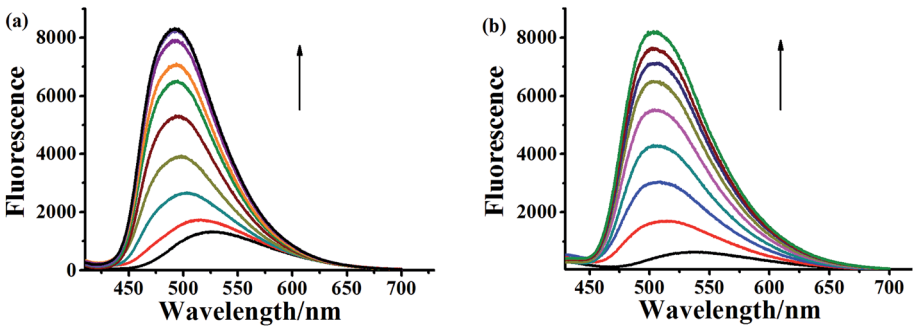

Fig. 4 Fluorescence spectral changes of compound **5a-1** (a) and **5a-2** (b) at the concentration of 3.0×10^{-5} M upon addition of CT DNA (arrow: 0–210 μM) in phosphate buffer (1 mM, pH 7.4) containing 20 mM NaCl at 25 °C.

binding mode and the interaction mechanism could be explained. Compounds **5a-1**, **5a-2**, **6a-1**, **6d-1** and **6b-3** were selected for the measurement of CD spectra at a certain ratio (*cf.* Fig. 5). Both data on the CD changes of DNA and ICD involving the tested compounds were obtained. In the absence of a drug, the CD spectrum of CT-DNA was of a typical B form, exhibiting a positive Cotton effect near 277 nm due to base staking and a negative Cotton effect near 247 nm due to polynucleotide helicity.[48] Upon addition of these selected compounds, the CD spectrum of the resulting DNA underwent an increase in both the positive and negative bands as shown in Fig. 5. The result give evidence of a mode of intercalation with DNA, since it is generally accepted that the classical intercalation enhances the base stacking and stabilizes helicity, and thus increases intensities of the both bands, whereas simple groove binding and electrostatic interaction of small molecules show less or no perturbation on the base stacking and helicity bands.[49]

Further evidence for the binding modes of these compounds was obtained from the ICD spectra in the range of 325–450 nm corresponding to an indoloquinoxaline chromophore. The ICD signal, displayed by these achiral molecules as a result of interaction with the chiral DNA, usually depends on the position and orientation with respect to the polynucleotide. Generally, adducts displaying intercalation binding characteristics were found to exhibit a positive or negative ICD.[50] Intriguingly, ICD spectra of the tested compounds and CT DNA exhibited a weaker and biphasic ICD signal. The biphasic shape of the CD spectrum, *i.e.* a negative band at lower wavelengths and a positive band at higher wavelengths, is characteristic of chromophores with a right-hand orientation, as expected for dyes bound to B-form DNA.[51] The exciton CD observed in the drug absorption region is generally considered as evidence of groove binding or external stacking.[44] However, the groove binding mode should be ruled out in this case due to the following consideration. Firstly, the ICD of groove binders is generally an order of magnitude stronger than those of intercalators and usually carries a positive sign if DNA is in B-form.[48,52] Secondly, in the absorption titration we have demonstrated that these drugs mixed with CT DNA still contain a partially free chromophore which did not interfere with the DNA helix. This in turn may be due to the notion that an external binding mode may exist simultaneously. Thirdly, considering the positive nature of these compounds and negatively charged polyphosphate skeleton of DNA, the electrostatic interactions between the intercalator and DNA has to be considered. Taken in concert, these results, together with light absorption characteristics, may suggest multiple binding modes including intercalation as major and external binding as minor mode.

2.4.4. Thermal denaturation. Thermal denaturation studies of CT DNA are useful to determine the ability of the present compound to stabilize double stranded DNA. The intercalation of small molecules into the double helix is known

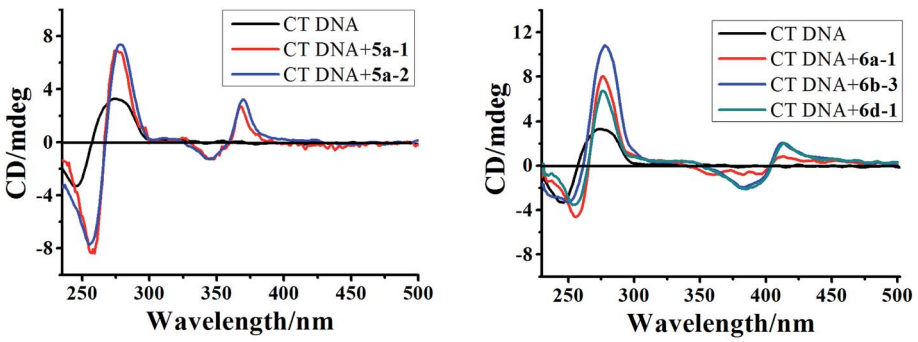

Fig. 5 CD spectra of CT DNA (6.0×10^{-5} M) in the absence and presence of **5a-1**, **5a-2**, **6a-1**, **6b-3** and **6d-1** (5.0×10^{-5} M) in phosphate buffer (1 mM, pH 7.4) containing 20 mM NaCl at 25 °C.

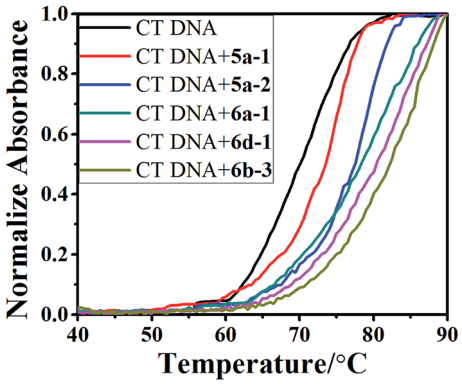

Fig. 6 DNA melting curves for CT DNA (5.0×10^{-5} M) in the absence and presence of **5a-1**, **5a-2**, **6a-1**, **6d-1** and **6b-3** with concentration of 5.0×10^{-6} M in phosphate buffer (1 mM, pH 7.4) containing 20 mM NaCl.

Table 6 Average T_m and ΔT_m for CT-DNA in the absence and presence of **5a-1**, **5a-2**, **6a-1**, **6b-3** and **6d-1**

Compound	T_m (°C)	ΔT_m (°C)
CT DNA	69.4	0
5a-1	73.5	4.1
5a-2	77.8	8.4
6a-1	79.3	9.9
6b-3	81.1	11.7
6d-1	80.2	10.8

to increase the DNA melting temperature (T_m). The T_m of DNA characterizes the transition from double-strand to single-strand nucleic acid.[53] DNA melting studies were carried out with CT DNA in the absence and presence of compound. The melting profile for CT DNA in the absence of compound was 69.4 °C. As shown in Fig. 6 and Table 6, under the same experimental conditions, the presence of compounds **5a-1** and **5a-2** increased the T_m value about 4.1 and 8.4 °C, while the T_m value for compounds **6a-1**, **6d-1** and **6b-3** increased 9.9, 10.8 and 11.7 °C, respectively. The dicationic quaternary ammonium salts derivatives possessed higher DNA melting temperatures than the corresponding mono quaternary ammonium salt derivatives. These results further indicate that compounds **6a-1**, **6d-1** and **6b-3** with methylation at 11-*N* exhibited strong affinities with CT DNA, consistent with the results obtained from UV-vis analysis. Taken in concert, the above results further emphasize that the novel 9-fluoro-6*H*-indolo[2,3-*b*]quinoxaline derivatives as DNA intercalators exhibited significant DNA binding affinities.

3. Conclusions

A series of novel 9-fluoro-6*H*-indolo[2,3-*b*]quinoxaline derivatives functionalized with amino side chains and their monocationic/dicationic quaternary ammonium salts were designed and synthesized and their interactions with CT DNA were studied. The incorporation of fluorine, alkyl amino side chains and the introduction of positive charge at 11-*N* position of the aromatic scaffold were found to significantly influence the antitumor activity and further demonstrated to enhance the binding affinity of the compounds with DNA. The antitumor activity and the DNA binding affinity of most of the synthesized quaternary dicationic FIQX derivatives were found to be significantly higher compared to the corresponding monocationic FIQX derivatives and the neutral 6*H*-indolo[2,3-*b*]quinoxaline derivatives. The synthesized dicationic FIQX derivatives with pyrrolidine or piperidinyl as terminal amino-groups exhibited a higher inhibitory activity. The molecular structure–DNA binding relationships assessed in this study may be useful for the design of 6*H*-indolo[2,3-*b*]quinoxaline derivatives with desired DNA binding properties and promising antitumor abilities.

4. Experimental section

4.1. Materials

All chemicals and reagents were of analytical grade. RPMI-1640 medium, trypsin and fetal bovine serum were purchased from Gibco (Grand Island, NY, USA). CT DNA, MTT, benzylpenicillin and streptomycin were purchased from Sigma-Aldrich (St. Louis, MO, USA). Three different human carcinoma cell lines, MCF-7, HeLa and A549, were obtained from American Type Culture Collection.

4.2. Instrumentation and measurements

The melting points were determined on an XT-4 microscopic melting-point spectrometer and are shown uncorrected. Elemental analysis was performed on an Elementar Vario EL III elemental analyzer. Infrared (IR) spectra were measured on a Perkin-Elmer Model-683 spectrophotometer, with samples analyzed as KBr pellets. The ^{1}H and ^{13}C NMR spectra were recorded on a Bruker AVIII 600 NMR spectrometer. Mass spectra were measured using an Agilent 1200-6310 LC-MS apparatus. High-resolution mass spectra (HRMS) were recorded on a Bruker Apex Ultra 7.0T FTMS mass spectrometer. UV-vis absorption spectra were recorded on a Shimadzu UV-3600 UV-vis spectrophotometer and fluorescent spectra were measured on a Hitachi F-7000 luminescence spectrophotometer. The optical density (OD) was measured on a microplate spectrophotometer (Bio-Rad Model 680, USA). The yield, IR, ^{1}H NMR, ^{13}C NMR and high-resolution electrospray ionization (HRESI) MS spectral data of the obtained compounds are provided in the ESI section.†

4.3. Synthesis of compounds

4.3.1. 9-Fluoro-6*H*-indolo[2,3-*b*]quinoxaline. A mixture of 5-fluoroisatin (10 g, 0.04 mol) and *o*-phenylenediamine (6.6 g, 0.05 mol) in acetic acid (100 mL) was refluxed with stirring for 5 h. The reaction mixture was then cooled to room temperature and neutralized with a saturated solution of sodium hydroxide to pH 7. The solid product was filtered off, washed with acetic acid (3–5 mL) and recrystallized from ethyl alcohol.

4.3.2. General procedure for preparation of series of compounds (3). To a stirred suspension of 9-fluoro-6*H*-indolo

[2,3-*b*]quinoxaline (2.39 g, 0.01 mol) in 30 mL of THF was added sodium hydroxide (2.81 g, 0.05 mol). The obtained solution was stirred for 30 min at 45 °C and dibromoalkane (0.05 mol) was added. After refluxing for 6 h, the reaction mixture was evaporated under reduced pressure and the residue was washed with water, filtered and dried. The product was purified by silica gel column chromatography using a mixture of petroleum ether and ethyl acetate as eluent.

4.3.3. General procedure for preparation of series of compounds (4). Cyclic secondary amine (10 mol) was added to a solution of compound **3** (1 mol) in 10 mL of THF. The reaction mixture was refluxed under nitrogen atmosphere until reaction completion as judged by TLC. The reaction mixture was then evaporated under reduced pressure and the residue was dissolved in 20 mL of water and extracted with ethyl acetate (3 × 15 mL). The extract was then neutralized with a saturated solution of sodium carbonate to pH 8–9 and the obtained precipitate was collected. The product was further purified by silica gel column chromatography using a mixture of petroleum ether and ethyl acetate as eluent.

4.3.4. General procedure for preparation of series of compounds (5). Iodomethane (1 mL) was added to a solution of compound **4** (0.5 mmol) in 5 mL of acetone under nitrogen atmosphere. The reaction mixture was stirred at room temperature until reaction completion as judged by TLC control. The precipitate was collected, washed with diethyl ether (3 × 5 mL) and dried.

4.3.5. General procedure for preparation of series of compounds (6). A suspension of compound **4** (0.5 mmol), iodomethane (2 mL) and tetramethylenesulfone (3 mL) was heated in a sealed flask overnight at 55 °C. The obtained clear, deep-red solution was cooled to room temperature. Next, 5 mL of water and 0.46 g of KPF_6 (2.5 mmol) was added and the mixture was stirred at 45 °C for 2 h. The resulted brick precipitate was filtered off, dried, and recrystallized from methanol.

4.3.6. Data collection and structural refinement of the precursor of compound 6b-1. X-ray data collection of the precursor of compound **6b-1** was performed on a Bruker SMART APEX II CCD diffractometer equipped with a graphite monochromator (Mo Kα radiation) (λ = 0.71073 Å) at 296(2) K. Multiscan absorption corrections were carried out using the SADABS program. The structure was solved by a direct method using the SHELXS-97 program. Refinements on F^2 were performed using SHELXL-97 by a full-matrix least-squares method with anisotropic thermal parameters for all non-hydrogen atoms. Crystallographic data for the structural analysis of the precursor of compound **6b-1** have been deposited at the Cambridge Crystallographic Data Centre, CCDC-1541589.†

4.4. Procedure for *in vitro* cytotoxictity assessment

In vitro cytotoxictity of the obtained compounds was evaluated by a MTT colorimetric assay.[54] Three different human carcinoma cell lines, MCF-7, HeLa and A549, were cultured in Dulbecco's modified Eagel's medium (DMEM, Gibco, USA) solution supplemented with 10% fetal bovine serum, 100 U mL^{-1} of penicillin, and 100 μg mL^{-1} of streptomycin. The cancer cells were seeded at a density of 1.5×10^4 cells per well into a 96-well microplate pre-incubated in a 5% CO_2/95% air-humidified atmosphere at 37 °C for 12 h to acquire adherent cells.

Prior to dilution, a stock solution of the compounds (5 mM) was prepared in DMSO. The 50% inhibitory concentration (IC_{50}) was determinated over a range of concentrations (0.1–100 μM). In all experiments, the concentration of DMSO was less than 0.1% (v/v) to avoid DMSO toxicity.

Wells containing culture medium without cells were used as blanks. Wells containing culture medium, FIQX and cisplatin were used as positive control. After incubation for 48 h with the test compounds, 20 μL of MTT solution (5 mg mL^{-1}) was added to each well and the mixtures were incubated for an additional 4 h. Then, 100 μL of DMSO was added to solubilize the MTT formazan and the OD of each well was measured on a microplate spectrophotometer at a wavelength of 570 nm. The IC_{50} value was determined from plot of the %-viability against a defined dose of added compounds. Three independent experiments were performed in quintuplicate.

4.5. Procedure for DNA binding studies

4.5.1. UV-vis absorption spectra. To prepare the stock solutions of calf thymus DNA (CT-DNA), DNA powder (Sigma-Aldrich) was dissolved in Tris–HCl buffer (pH 7.4; concentration 10 mM) and the solutions were incubated at 4 °C for 12 h. The DNA solution showed a ratio of UV absorbance at 260 and 280 nm, A260/A280 of approximately 1.9, indicating that the DNA was sufficiently free of protein. The concentration of CT DNA was determined by measuring its absorption intensity at 260 nm with a known molar absorption coefficient value of 6600 M^{-1} cm^{-1}. The selected compounds were dissolved in DMSO and diluted with Tris–HCl buffer to reach the required concentrations. Absorption spectra titration studies were performed by keeping the compound concentrations constant while varying the DNA concentrations at room temperature. Absorption spectra were recorded from 200 to 600 nm, and changes on the intensity of the bands were monitored. The titration processes were repeated until no spectral changes for at least four titrations could be observed, indicating that binding saturation was achieved.

4.5.2. Fluorescent spectra. Fluorescence absorption spectral studies were performed by keeping the compound concentration (30 μM) constant while varying the DNA concentration from 0 μM to 210 μM at room temperature. The fluorescence wavelength and intensity area of the samples were measured by the excitation wavelength at 360 nm.

4.5.3. Circular dichroism spectra. CD spectra of CT DNA modified by **5a-1**, **5a-2**, **6a-1**, **6d-1** and **6b-3** were recorded at 25 °C in 25 mmol L^{-1} sodium phosphate buffer (pH = 7.4) by using a MOS-450 spectrophotometer (Bio-Logic, France) equipped with a thermoelectrically controlled cell holder with a cell path length of 1 cm. CD spectra were recorded by keeping the DNA concentration (60 μM) constant while varying the compound concentrations until no spectral changes for at least three titrations in the region of 200–500 nm could be observed. The spectrum of the corresponding buffer and of the

compounds alone were also collected and subtracted from that of the reaction mixture.

4.5.4. DNA thermal denaturation. Thermal denaturation experiments were carried out on a Shimadzu UV-3600 spectrophotometer equipped with a high performance temperature controller (±0.1 °C). The melting temperature (T_m) was determined as the mid-point of the hyperchromic transition. The DNA (50 μM) was denatured by increasing the temperature from 35 to 90 °C at a speed of 1 °C min^{-1} in the presence and absence of compound **5a-1**, **5a-2**, **6a-1**, **6d-1** and **6b-3** (5 μM) while the corresponding absorbance was monitored at 260 nm. The data were presented as $(A - A_0)/(A_f - A_0)$ *versus* temperature, where A, A_0, and A_f are the observed, the initial, and the final absorbance at 260 nm, respectively.

Conflicts of interest

There are no conflicts to declare.

Acknowledgements

This work was supported by the Nature Science Fund of Hebei Province (B2015201213, B2015201069), the Key Basic Research Special Foundation of Science Technology Ministry of Hebei Province (15962602D), the Key Research Project Foundation of Department of Education of Hebei Province (Grant No. ZH2012041).

References

1 R. L. Siegel, K. D. Miller and A. Jemal, Cancer Statistics, *Ca-Cancer J. Clin.*, 2015, **65**, 5–29.
2 B. G. Jackson, *Science*, 2000, **287**, 1969–1973.
3 American Cancer Society, Inc., Surveillance Research. Cancer Faiths and Figures, 2005, http://www.geocites.com.
4 J. Fischer and C. R. Ganellin, *Analogue-based drug discovery*, Wiley-VCH, Weinheim, 2006, pp. 1–24.
5 X. B. Zhou, M. Chen, Z. Y. Zheng, G. Y. Zhu, Z. H. Jiang and L. P. Bai, *RSC Adv.*, 2017, **7**, 26921–26929.
6 B. Zhang, R. Y. Guo, Y. Z. Hu, X. W. Dong, N. M. Lin, X. Y. Dai, H. H. Wu, S. L. Ma and B. Yang, *RSC Adv.*, 2017, **7**, 31899–31906.
7 Y. Chen, H. Z. Lin, J. Zhu, K. Gu, Q. Li, S. Y. He, X. Lu, R. X. Tan, Y. Q. Pei, L. Wu, Y. Y. Bian and H. P. Sun, *RSC Adv.*, 2017, **7**, 33851–31867.
8 T. Zawadowski and M. Klimaszewska, *Acta Pol. Pharm.*, 1995, **52**, 249–252.
9 S. T. Hazeldine, L. Polin, J. Kushner, K. White, T. H. Corbett and J. P. Horwitz, *Bioorg. Med. Chem.*, 2006, **14**, 2462–2467.
10 P. J. Aragon, A. D. Yapi, F. Pinguet, J. M. Chezal, J. C. Teulade and Y. Blache, *Chem. Pharm. Bull.*, 2007, **55**, 1349–1355.
11 L. M. Wilhelmsson, N. Kingi and J. Bergman, *J. Med. Chem.*, 2008, **51**, 7744–7750.
12 N. S. H. N. Moorthy, E. Manivannan, C. Karthikeyan and P. Trivedi, *Mini-Rev. Med. Chem.*, 2013, **13**, 1415–1420.
13 N. S. H. N. Moorthy, C. Karthikeyan and P. Trivedi, *J. Enzyme Inhib. Med. Chem.*, 2010, **25**, 394–405.
14 M. Stiborová, J. Poljaková, E. Martínková, L. Borek-Dohalska, T. Eckschlager, R. Kizek and E. Frei, *Interdiscip. Toxicol.*, 2011, **4**, 98–105.
15 A. M. A. Osman, E. B. Pedersen and J. Bergman, *Nucleosides, Nucleotides Nucleic Acids*, 2013, **32**, 98–108.
16 N. Patel, J. Bergman and A. H. Gräslund, *Eur. J. Biochem.*, 1991, **197**, 597–604.
17 I. Zegar, A. Gräslund, J. Bergman, M. Eriksson and B. Nordén, *Chem.-Biol. Interact.*, 1989, **72**, 277–293.
18 J. Bergman, C. Damberg and H. Valberg, *Recl. Trav. Chim. Pays-Bas*, 1996, **115**, 31–36.
19 U. Sehlstedt, P. Aich, J. Bergman, H. Vallberg, B. Nordén and A. Gräslund, *J. Mol. Biol.*, 1998, **278**, 31–56.
20 J. Harmenberg, A. Åkesson-Johansson, A. Gräslund, T. Malmfors, J. Bergman, B. Wahren, S. Åkerfeldt, L. Lundblad and S. Cox, *Antiviral Res.*, 1991, **15**, 193–204.
21 K. Hirata, J. Araya, S. Nakaike, K. Kitamura and T. Ishida, *Chem. Pharm. Bull.*, 2001, **49**, 44–48.
22 T. Ishida, Y. Mihara, Y. Hama, A. Hanatani, M. Tarui, M. Doi, S. Nakaike and K. Kitamura, *Chem. Pharm. Bull.*, 1998, **46**, 739–743.
23 S. P. Nikumbh, A. Raghunadh, V. N. Murthy, R. Jinkala, S. C. Joseph, Y. L. N. Murthy, B. Prasad and M. Pal, *RSC Adv.*, 2015, **5**, 74570–74574.
24 S. P. Nikumbh, A. Raghunadh, T. S. Rao, V. N. Murthy, S. C. Joseph, Y. L. N. Murthy and M. Pal, *RSC Adv.*, 2016, **6**, 23489–23497.
25 K. W. Hagmann, *J. Med. Chem.*, 2008, **51**, 4359–4369.
26 S. S. Karki, R. Hazare, S. Kumar, V. S. Bhadauria, J. Balzarini and E. De Clercq, *Acta Pharm.*, 2009, **59**, 431–440.
27 M. F. Braña, M. Cacho, A. Gradillas, B. de Pascual-Teresa and A. Ramos, *Curr. Pharm. Des.*, 2001, **7**, 1745–1780.
28 D. Monchaud and M. P. Teulade-Fichou, *Org. Biomol. Chem.*, 2008, **6**, 627–636.
29 G. W. Gribble, Synthesis and antitumor activity of ellipticine alkaloids and related compounds, in *The Alkaloids*, ed. A. Brossi, Academic Press, New York, 1990, vol. 39, pp. 239–343.
30 V. K. Kansal and P. Potier, *Tetrahedron*, 1986, **32**, 2389–2408.
31 M. O. Shibinskaya, S. A. Lyakhov, A. V. Mazepa, S. A. Andronati, A. V. Turov, N. M. Zholobak and N. Y. Spivak, *Eur. J. Med. Chem.*, 2010, **45**, 1237–1243.
32 M. O. Shibinskaya, A. S. Karpenko, S. A. Lyakhov, S. A. Andronati, N. M. Zholobak, N. Y. Spivak, N. A. Samochina, L. M. Shafran, M. J. Zubritsky and V. F. Galat, *Eur. J. Med. Chem.*, 2011, **46**, 794–798.
33 P. B. Arimondo, B. Baldeyrou, W. Laine, C. Bal, F. A. Alphonse, S. Routier, G. Coudert, J. Y. Mérour, P. Colson, C. Houssier and C. Bailly, *Chem.-Biol. Interact.*, 2001, **138**, 59–75.
34 M. O. Shibinskaya, N. A. Kutuzova, A. V. Mazepa, S. A. Lyakhov, S. A. Andronati, M. J. Zubritsky, V. F. Galat, J. Lipkowski and V. C. Kravtsov, *J. Heterocycl. Chem.*, 2012, **49**, 678–682.
35 K. M. Driller, S. Libnow, M. Hein, M. Harms, K. Wende, M. Lalk, D. Michalik, H. Reinke and P. Langer, *Org. Biomol. Chem.*, 2008, **6**, 4218–4223.

36 M. C. Wamberg, A. A. Hassan, A. D. Bond and E. B. Pedersen, *Tetrahedron*, 2006, **62**, 11187–11199.
37 S. Avula, J. R. Komsani, S. Koppireddi, R. Yadla, A. K. R. Kanugula and S. Kotamraju, *Med. Chem. Res.*, 2013, **22**, 3712–3718.
38 A. H. Abadi, *Arch. Pharm.*, 1998, **331**, 352–358.
39 J. H. Tan, Q. X. Zhang, Z. S. Huang, Y. Chen, X. D. Wang, L. Q. Gu and J. Y. Wu, *Eur. J. Med. Chem.*, 2006, **41**, 1041–1047.
40 X. Q. Chen and J. M. Gu, *App. Chem. Ind.*, 2007, **36**, 901–902.
41 V. Q. Yen, N. P. Buu-Hoi and N. D. Xuong, *J. Org. Chem.*, 1958, **23**, 1858–1861.
42 P. Helissey, S. Desbene-Finck and S. Giorgi-Renault, *Eur. J. Org. Chem.*, 2005, 410–415.
43 Z. F. Chen, S. P. Zhang, J. Zhang and Z. Z. Zhu, *New J. Chem.*, 2017, **41**, 6760–6768.
44 S. J. T. Rezaei, V. Amani, M. R. Nabid, N. Safari and H. Niknejad, *Polym. Chem.*, 2015, **6**, 2986.
45 R. Raveendran, J. P. Braude, E. Wexselblatt, V. Novohradsky, O. Stuchlikova, V. Brabec, V. Gandin and D. Gibson, *Chem. Sci.*, 2016, **7**, 2381–2391.
46 Y. J. Lu, T. M. Ou, J. H. Tan, J. Q. Hou, W. Y. Shao, D. Peng, N. Sun, X. D. Wang, W. B. Wu, X. Z. Bu, Z. S. Huang, D. L. Ma, K. Y. Wong and L. Q. Gu, *J. Med. Chem.*, 2008, **51**, 6381–6392.
47 R. Palchaudhuri and P. J. Hergenrother, *Curr. Opin. Biotechnol.*, 2007, **18**, 497–503.
48 J. H. Tan, Y. J. Lu, Z. S. Huang, L. Q. Gu and J. Y. Wu, *Eur. J. Med. Chem.*, 2007, **42**, 1169–1175.
49 M. V. Keck and S. J. Lippard, *J. Am. Chem. Soc.*, 1992, **114**, 3386–3390.
50 P. Pradhan, B. Jernström, A. Seidel, B. Nordén and A. Gräslund, *Biochemistry*, 1998, **37**, 4664–4673.
51 K. M. Sovenyhazy, J. A. Bordelon and J. T. Petty, *Nucleic Acids Res.*, 2003, **31**, 2561–2569.
52 B. Norden and T. Kurucsev, *J. Mol. Recognit.*, 1994, **7**, 141–156.
53 Y. Cao and X. W. He, *Spectrochim. Acta, Part A*, 1998, **54**, 883–892.
54 T. Mosmann, *J. Immunol. Methods*, 1983, **65**, 55–63.